Sticking of droplets on slippery superhydrophobic surfaces by laser induced forward transfer

Christos Boutopoulos, Dimitrios P. Papageorgiou, Ioanna Zergioti, and Athanasios G. Papathanasiou

Additional information on Appl. Phys. Lett.
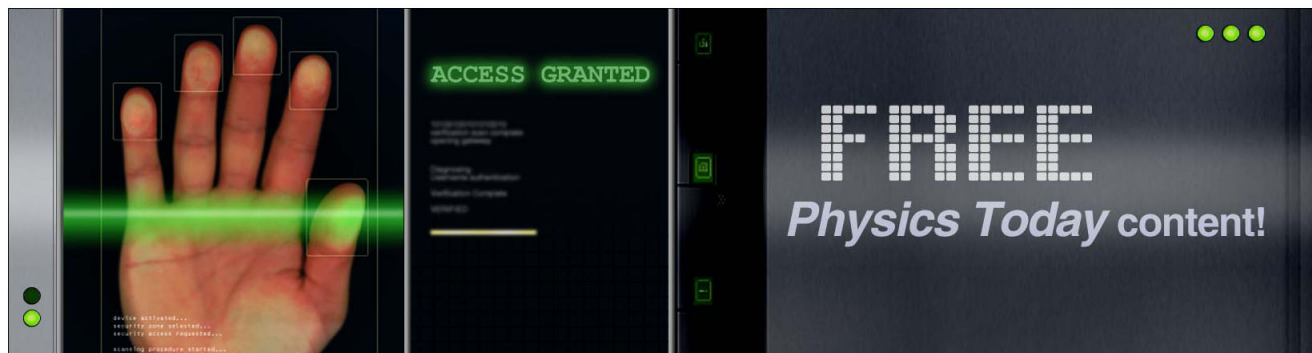
Sticking of droplets on slippery superhydrophobic surfaces by laser induced forward transfer

Christos Boutopoulos,[1,a)] Dimitrios P. Papageorgiou,[2] Ioanna Zergioti,[1] and Athanasios G. Papathanasiou[2,b)]

[1]School of Applied Mathematical and Physical Sciences, National Technical University of Athens, GR-15780 Athens, Greece
[2]School of Chemical Engineering, National Technical University of Athens, GR-15780 Athens, Greece

Liquid jets created by the Laser Induced Forward Transfer (LIFT) technique can reach extremely high speeds exceeding 270 m/s. The impact of such a jet on a solid surface can create a dynamic pressure of 35 MPa, enabling the LIFT process to stick liquid droplets on highly slippery superhydrophobic surfaces. In this letter, we demonstrate how LIFT printing can be utilized in order to achieve selective sticky behavior on slippery surfaces, valuable for many biosensor applications, and we suggest it as a tool of evaluating the thermodynamic robustness of the so called Fakir states on various rough hydrophobic surfaces. © 2013 AIP Publishing LLC. [http://dx.doi.org/10.1063/1.4813394]

The combination of suitable roughness morphology (micro-/nano surface texture) and material hydrophobicity may lead to water repelling surfaces, mimicking the lotus effect,[1] which display contact angles (CAs) greater than 150° accompanied by very low contact angle hysteresis (CAH). In some cases, the superhydrophobic (SH) effect (connected with the thermodynamic robustness of a superhydrophobic surface) is so pronounced that even low surface tension liquids ($\gamma_{lv} = 15$–50 mN/m) are easily repelled, and the surfaces are commonly called superoleophobic or omniphobic.[2–4] Their attractive properties led to commercial interest for a broad range of applications, such as liquid drag reduction in microfluidic channels,[5] self-cleaning,[6,7] liquid-repellent textiles,[8,9] and microbatteries.[10]

Liquid drops deposited on such surfaces ideally sit on top of the roughness features (micro pillars, micro needles); however, this state (often called "Fakir" state) is often meta-stable, i.e., the drop may get partially or fully impaled by the roughness protrusions. Liquid drop impalement, i.e., liquid sticking, could be actively triggered by mechanical or electrical actuation such as squeezing,[11,12] impact from a height,[13] electrowetting,[3,14,15] etc. The resistance that a SH surface shows to liquid drop impalement is directly connected to the maximum surface pressure, P_{crit}, that induces impalement[15] and this pressure is correlated to its thermodynamic robustness. The conventional techniques, mentioned above, that could determine P_{crit} fail to apply pressures higher than ~50 kPa. However, appropriately engineered surfaces could, in principle, sustain a pressure of few MPa prior to water drop impalement.[16,17]

Laser Induced Forward Transfer (LIFT) enables the controlled transfer of a thin film of a liquid or solid material, from a donor substrate to a receiving substrate by means of pulsed laser irradiation.[18] A typical liquid phase LIFT donor substrate consists of a transparent carrier covered by a thin radiation absorption layer on which the liquid film has been applied. The liquid material ejection is initiated by the generation of a high pressure vapor pocket at the radiation absorbing layer–liquid film interface due to the localized laser energy delivery. The expansion of the vapor pocket generates a dynamic jet that reaches the receiving substrate with a high impact velocity (see Figure 1). A lot of research effort has been directed towards the optimization of the LIFT process of liquid solutions in the last years. The effect of several experimental parameters (i.e., laser fluence, laser pulse duration, solution properties, etc.) on the deposition dynamics[19,20] and printing quality[21] has been extensively investigated using hydrophilic receiving substrates. However, there is a lack of studies for the deposition dynamics and the potential applications of the technique when superhydrophobic receiving substrates are used.

Here, we propose the use of the LIFT technique to trigger impalement transitions on superhydrophobic surfaces through the generation of extremely high jet impact velocities (up to ~270 m/s). This way, droplets are easily deposited and sticked even on highly robust and slippery superomniphobic surfaces. Considering the jet velocity range, 10 to 270 m/s that LIFT is able to achieve, the calculated range of the resulting dynamical pressures is ~50 kPa to ~35 MPa, i.e., almost 30 times higher than the pressures attained with other conventional methods (e.g., the maximum impact pressure for conventional ink jet printing is about 1 MPa). The jet creation and impact dynamics is presented through a time-resolved imaging of the LIFT process, which allowed for the investigation of the liquid deposition dynamics involved in various wetting states. The proposed LIFT-induced deposition of liquids is important for biosensing applications since it can lead to direct immobilization of biomolecules even on rough hydrophobic sensing substrates.[22,23]

The LIFT setup (shown in Figure 1) consists of a pulsed Nd:YAG laser (neodymium-doped yttrium aluminum garnet, 266 nm wavelength, 10 ns pulse duration) and a mask projection optical setup, described in detail elsewhere.[24] The laser spot size at the donor substrate was 130 μm and the laser

a)Present address: Department of Engineering Physics, Laser Processing and Plasmonics Laboratory, École Polytechnique de Montréal, CP6079 Succ. Centre-ville, Montréal, H3C 3A7 Québec, Canada
b)Author to whom correspondence should be addressed. Electronic mail: pathan@chemeng.ntua.gr. Tel.: +30 210 7723234. Fax: +30 210 7723298
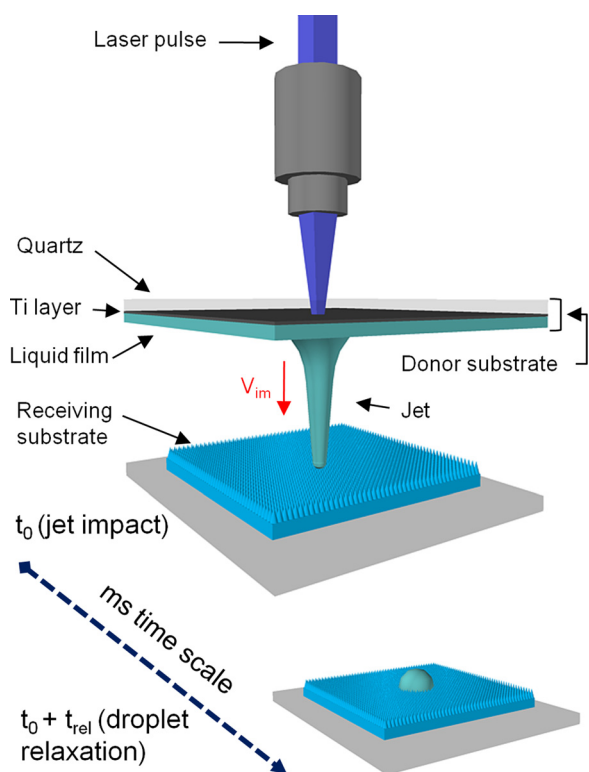
FIG. 1. Sketch of the main parts of the LIFT setup, no to scale. Each laser pulse creates a high velocity liquid jet which collides against the receiving substrate. The resulting droplet, past relaxation time, is shown at the bottom.

fluence was systematically adjusted in the range of 150–1300 mJ/cm^2 (150 mJ/cm^2 was the fluence threshold value sufficient for the liquid jet formation). The distance between the donor and the receiving substrate was kept fixed at 330 μm. The liquid solution (test liquid) used in the current study was a 1.0 M potassium phosphate buffer (0.5 M KH$_2$PO$_4$, 0.5 M K$_2$HPO$_4$, pH 8), plus the sodium dodecyl sulfate surfactant diluted at a concentration of 2.0 mg/ml. The measured viscosity, η, and the surface tension, γ_{lv}, of the test liquid were equal to 1.15 mPa s and 34 mN/m, respectively. The donor substrates were prepared by drop casting 30 μl of the liquid solution on to 1-in. quartz plates coated with a 40-nm titanium laser-absorbing layer. This resulted to the formation of liquid film with a thickness of about 60 μm on the quartz substrate. The laser induced transfer was performed in such a way that each liquid jet was created on the donor and subsequently collided on the receiving surface by the action of a single laser pulse.

The ultrafast jetting and impact dynamics, involved in LIFT process, could not be captured by conventional high speed cameras, which are usually employed to study low velocity impact of droplets on SH surfaces. Therefore, side view imaging of the dynamic evolution of the liquid jet impact was performed using an appropriate time-resolved imaging setup. Time-resolved imaging was based on a pump-probe experimental methodology, which allowed for capturing snapshots of the ultrafast jetting dynamics with nanosecond temporal resolution. In particular, a second probe laser (Nd:YAG, 532 nm wavelength, 10 ns pulse duration) was used for back side incoherent illumination of each LIFT event by pumping a fluorescence dye (rhodamine). A pulse delay generator was used to control the delay between

the pump (LIFT) and probe (illuminating) laser pulses. Shadowgraphic images were captured by a CCD camera (Unibrain 810c), also triggered by the pulse delay generator. Processing the acquired side view images using edge detection software enabled the calculation of the jet velocity, u$_{jet}$, just before the impact to the surface. The resulting impact pressure was calculated by the following relation: $P_{im} = \frac{1}{2}\rho \cdot u_{jet}^2$, where u_{jet} is the impact velocity of the liquid and ρ is the density of the liquid.[25]

The tested SH substrates were prepared by oxygen plasma etching followed by fluorocarbon plasma deposition on 2 mm thick poly(methyl methacrylate) (PMMA) substrates, which produce hierarchical randomly rough SH surfaces. The PMMA SH substrates preparation and surface characterization are described by Gnanappa *et al.*[12] Figure 2 shows Scanning Electron Microscopy (SEM) images of 4 min and 10 min oxygen plasma etched nanotexture PMMA surfaces tested in this work. Surface roughness protrusions range in mean diameter from 60 nm to 150 nm, in spacing from 100 to 500 nm, and in height from 500 nm to 1600 nm.

Estimation of the roughness factor, r = (actual surface area)/(projected surface area), by considering Gaussian protrusion profile gave r ~ 1.5 for the 4 min and r ~ 1.7 for the 10 min oxygen plasma etched nanotexture, respectively.

Static CA measurements were performed by processing the side view snapshots of sessile droplets using an in house built drop shape analysis setup.[26] Pipette deposited droplets were about 2 μl in volume, while the LIFT deposited droplets' volume ranged from 2.6 nl to 3 nl for laser fluence ranging from 150 mJ/cm^2 to 1300 mJ/cm^2. CAH measurements (where needed) were performed by increasing (advancing CA) or decreasing (receding CA) the droplet volume using a computer controlled syringe pump; the CAH is obtained from the difference between the advancing and receding CA values.

The two selected surfaces tested, namely the ones shown in Figure 2, showed remarkable resistance to the impalement transition.[12] Both surfaces could easily sustain Cassie states, i.e., no impalement was observed, for water (γ_{lv} = 72 mN/m) and diiodomethane (γ_{lv} = 50 mN/m) droplets mechanically pressed with pressures of 1.5 kPa,[12] the limit of the pressurizing technique. No impalement was also observed for free falling droplets from a height of 1.5 m, i.e., a test similar to the one shown by Brunet *et al.*[27] This test generated an impact speed of 5.5 m/s and the corresponding dynamical pressure was estimated to be around 17 kPa. Our LIFT setup was capable of generating high speed liquid jets resulting to
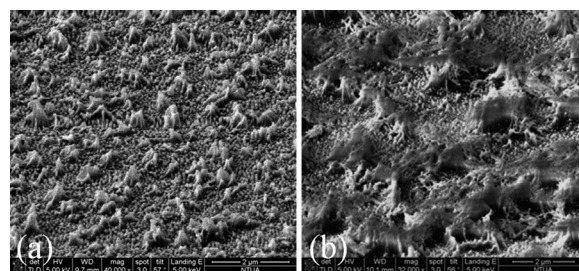

FIG. 2. SEM pictures of (a) 4 min and (b) 10 min oxygen plasma etched nanotexture PMMA surfaces, respectively. Both surfaces were coated by plasma-deposited fluorocarbon films.

dynamical pressures up to 35 MPa, depending of the laser fluence adjustment.

Pipette deposited droplets (of the test liquid) demonstrated CA of 152° and 157° on the 4 min and 10 min etched surfaces, respectively, with no indication of pinning. In the case of smooth surfaces, the CA was measured to be $\theta = 85° \pm 3°$ and $105° \pm 3°$ for a surface coated by a plasma deposited fluoropolymer (C_4F_8) and by spin coated Teflon, respectively. Notice that plasma coated fluoropolymer was used for coating the tested rough surfaces. The CA, for LIFT-printed droplets, was slightly lower (~150°) for laser fluence up to 400 mJ/cm^2, corresponding to a dynamical pressure of 400 kPa (see Figure 3(a)). In particular, for the 4 min etched surface and for laser energies lower than 400 mJ/cm^2, the droplets pinned at the surface despite the high contact angle, demonstrating the so called rose-petal effect.[28]

The pinning was so strong that the droplet stayed sticked even if the surface was turned upside down. Further increase of the laser fluence up to 900 mJ/cm^2 (corresponding to dynamical pressure of 20 MPa) resulted in a progressive decrease of the CA of the printed droplets down to $90° \pm 5°$, reaching a lower limit for the surface studied. The observed CA is slightly higher than the one, θ_w, computed by the Wenzel[29] relation

$$\cos\theta_w = r\cos\theta_y. \tag{1}$$

(a)

In particular, Eq. (1) gives $\theta_w = 82.5°$ for r = 1.5 and $\theta_y = 85°$.

Droplets rolled off when relatively low laser fluence (150 mJ/cm^2–250 mJ/cm^2) LIFT was performed on the 10 min etched surface (Figure 3(b)). Consequently, measuring of contact angle was not possible since the droplets were bounced out from the target surface and possibly incorporated into the liquid donor film. The threshold laser fluence for pinning, i.e., sticking, of the LIFT printed droplets on the 10 min etched surface was 300 mJ/cm^2. The corresponding dynamical pressure was ~160 kPa and the measured CA was 140°, as shown in Figure 3(b). Notice that this high pressure is neither achievable by conventional pressurizing tests nor by droplet impact tests presented so far.[30] For instance, a rain droplet (maximum speed of the order of 10 m/s, depending on droplet size) induces dynamic pressure of ~100 kPa during the impact. Here, on one hand, the ability of the LIFT technique to create high speed droplets is demonstrated, and on the other hand, the valuable advantage of the particular studied surface (i.e., the 10 min etched surface) to withstand impalement transitions is presented. As also observed in the 4 min etched surface, the CA of the LIFT printed droplet decreased progressively reaching a lower limit of $110° \pm 7°$, which is considerably higher than the CA calculated by Eq. (1). Indeed, the Wenzel angle, θ_w, is computed to be equal to 81.5° for r = 1.7 and $\theta_y = 85°$. The difference between the minimum CA and the θ_w was indicative of partial wetting state even for high dynamic pressures. Indeed, the dynamic pressure takes its maximum value at the jet impact point, while the lateral liquid flow results in a decreased wetting pressure at the periphery due to the conversion of the elastic energy of the compressed liquid to kinetic energy.[25] As a result, the droplets eventually present the so-called partial wetting state.[17]

The dynamics of LIFT printing on a 4 min etched surface (shown in Figure 2(a)) is presented for two series of experiments, namely for low and high laser fluence, respectively. In Figure 4(a), where the laser fluence is 300 mJ/cm^2, the creation of the jet was followed by a fast formation of a liquid bridge connecting the donor (here shown as the lower surface) and the receiving test surface (here shown as the upper surface). The calculated liquid front velocity was 18 m/s corresponding to an impact pressure of 160 kPa. Past the initial impact with the upper substrate and the subsequent formation of several satellite droplets, a continuous liquid feeding process takes place.[19,31] Then, the liquid bridge was broken probably due to the high liquid momentum. The observed dynamics for the low laser fluence LIFT is in agreement with the observation of Deng *et al.*[17] for droplet impact on a fluorinated silicon nanowire surface, where the main droplet recoiled and completely bounced off the surface. The resulting main droplet, of volume of about 3 nl, bounced back and forth between the solid surfaces. Finally, the droplet was pinned and relaxed on the receiving substrate after ~1 ms, having a CA of 150°. Such bouncing dynamics has not been reported in previous studies dealing with LIFT of liquid solutions, possibly due to the hydrophilic substrates used so far. Presumably hydrophilic substrates favor stronger pining than the superhydrophobic ones tested here.

On the other hand, for considerably higher laser fluence (930 mJ/cm^2), completely different dynamics was observed.
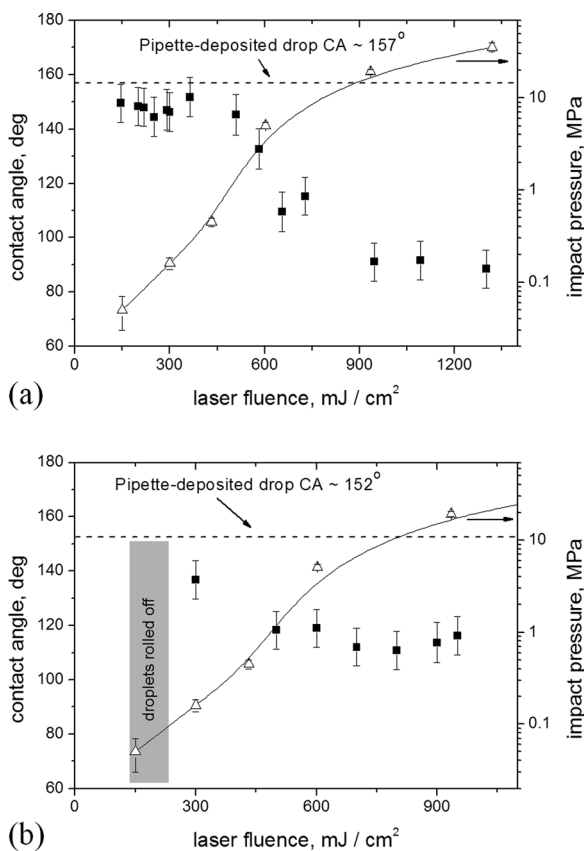

(b)

FIG. 3. Dependence of the LIFT-printed drop CA (left axis, filled square markers) on the laser fluence on (a) 4 min and (b), 10 min oxygen plasma etched nanotexture PMMA, respectively. The dashed lines in (a) and (b) depict the CA value of a pipette-deposited drop. The gray marked area in (b) corresponds to a laser fluence range (150 mJ/cm^2 to 250 mJ/cm^2), where the droplets bounced away from the target surface. The calculated values of the droplet dynamical pressures are depicted with empty triangular markers (read at the right axes). Solid lines are drawn as guide to the eye.
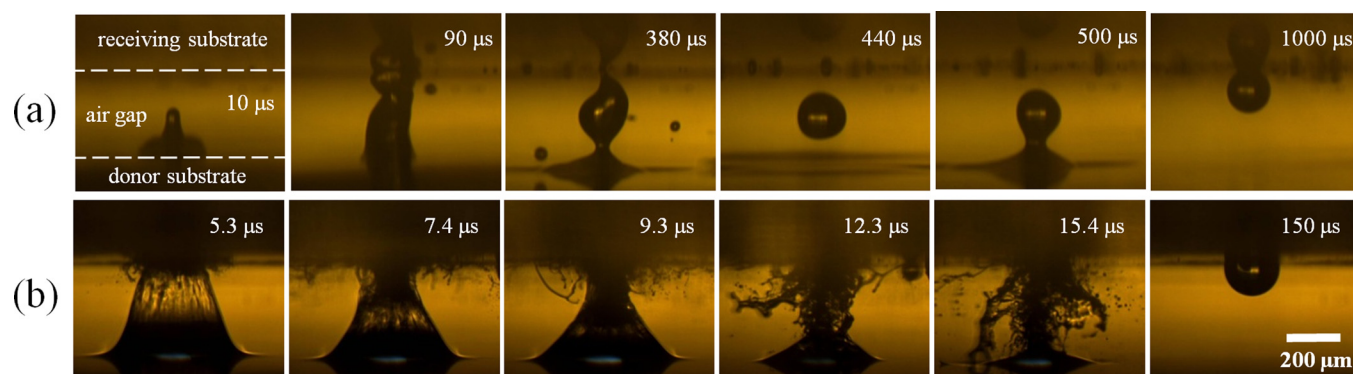
FIG. 4. Side view imaging of the evolution of LIFT printing on the superhydrophobic substrate shown in Figure 2(a) (a) for low (300 mJ/cm^2) and (b) for high (930 mJ/cm^2) laser fluence, respectively. Representative snapshots are presented.

The liquid front velocity was calculated as ~200 m/s. The high laser energy resulted in an immediate formation of an almost conical liquid bridge connecting the donor and the receiving test surface. The liquid front collision on the test surface created debris like dispersion of microdroplets and then the created bridge collapsed and equilibrated, pinned, solely at the receiving surface. The measured CA of 90° was considerably lower than the one of the pipette deposited droplets on such surface (see also Figure 3(a)), showing the remarkable effect of forced pinning induced by LIFT especially if the laser energy is high. It is worth clarifying that, when droplet sticking is observed, and especially when accompanied by a considerable decrease of the contact angle (full impalement), i.e., for high laser energies, no liquid rebound was noticed. In particular, for the experiment shown in Figure 4(b), the droplet remains sticked at the upper surface ~150 μs past the impact (see last snapshot in Figure 4(b)). On the contrary, when no considerable decrease of the contact angle is observed, i.e., at low laser energies, the droplet bounces between the two surfaces before it sticks since no full impalement is achieved (see snapshots in Figure 4(a)).

A thorough study of the dynamics is out of the scope of this letter; however, it remains a challenge to study the possible connection between roughness features and the jet shape evolution in such small time scales (order of μs), where traditional high speed video capturing is not applicable.

Forced and selective immobilization of droplets with biological content is important in biosensor applications. Such a study has been performed by Boutopoulos *et al.*,[23] where LIFT was employed to immobilize a photosynthetic bio content (i.e., solution of thylakoid membranes) on a gold amperometric sensor substrate. In particular, thylakoid membranes deposited by LIFT on gold sensors' surface generated relative high electric current (~300 nA) upon to their illumination, indicating enhanced immobilization even under continuous flow measurement conditions. In contrast, the reference pipette deposited thylakoid droplets were easily removed by rinsing. The perfect LIFT induced immobilization on the sensor surfaces was attributed to the impalement of the liquid to the roughness protrusions (~0.5 μm rms roughness) of the gold sensor surface. Here, indicatively, we present LIFT of biomaterial droplets on rough (~0.5 μm rms roughness) hydrophobic (pipette-deposited CA ~89.0°) graphite electrodes. The tested biomaterial solution was prepared by dissolving Laccase enzyme (40 Units/100 μl) in PBS (Phosphate Buffered Saline, 37 mM NaCl, 2.7 mM KCl, 10 mM Na$_2$HPO$_4$O, 2 mM KH$_2$PO$_4$O, pH 4.5). As it can be seen in Figure 5, LIFT affects the CA of the printed droplet for laser fluences that are higher than 170 mJ/cm^2. Even higher laser fluence results in a considerable decrease of the CA, reaching a lower limit of 20° accompanied by a strong immobilization of the printed droplets and the biological content, also confirmed by standard amperometric measurements under flow conditions (i.e., using the protocol described by Scognamiglio *et al.*[32]).

Summarizing, we used LIFT technique to create high speed liquid jets against highly robust water-repellent superhydrophobic surfaces and create forced and strong droplet sticking on them, due to the high dynamical pressure. Imaging the jet dynamics with time resolved-imaging, we showed the basic aspects of the droplet impact on the superhydrophobic surfaces studied for low and high laser energies. Finally, we printed droplets carrying bio content (Laccase enzyme in PBS buffer) on graphite sensor electrode surface and we observed strong enzyme immobilization on the electrode. Our data showed mainly that roughness is a primary factor that affects immobilization of biological content on surfaces. We prepared almost perfectly flat and smooth spin coated Teflon surfaces and we performed LIFT printing on them. We observed that the CA of the printed droplets remained unaltered even at very high laser energies, up to
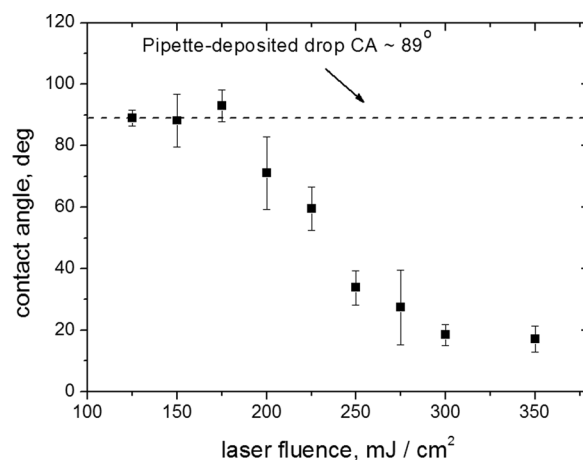

FIG. 5. Dependence of the LIFT-printed drop CA on the laser fluence on graphite electrode surface.

1300 mJ/cm^2, and equal to the CA of the pipette deposited droplet, namely $105° \pm 3°$. The thorough understanding of the combined effect of roughness and surface material on the immobilization of biological content on sensor surfaces is under current investigation by our group.

In conclusion, LIFT printing is shown to be a valuable tool for the exploration of liquid jet impact dynamics on solid surfaces. Many technological applications can be benefited, like turbine technology in aircraft or steam power plants where droplets can build up pressures of the order of MPa. The ability to stick droplets even on highly slippery superhydrophobic surfaces, like the ones tested in this work, renders LIFT technique as a valuable tool not only for testing the thermodynamic robustness of the superhydrophobic surfaces (in terms of maximum pressure for sustaining slippery behavior) but also for creating selective sticking/immobilization for biosensor applications where certain bio substances must be strongly bind to solids and withstand various flow conditions.

[1]W. Barthlott and C. Neinhuis, Planta **202**(1), 1 (1997).

[2]A. Tuteja, W. Choi, J. M. Mabry, G. H. McKinley, and R. E. Cohen, Proc. Natl. Acad. Sci. U.S.A. **105**(47), 18200 (2008).

[3]A. Ahuja, J. A. Taylor, V. Lifton, A. A. Sidorenko, T. R. Salamon, E. J. Lobaton, P. Kolodner, and T. N. Krupenkin, Langmuir **24**(1), 9 (2008).

[4]T. Wu and Yi Suzuki, Sens. Actuators B **156**(1), 401 (2011).

[5]D. P. Papageorgiou, K. Tsougeni, A. Tserepi, and E. Gogolides, Microfluid. Nanofluid. **14**(1–2), 247 (2013).

[6]A. Marmur, Langmuir **20**(9), 3517 (2004).

[7]N. A. Patankar, Langmuir **20**(19), 8209 (2004).

[8]B. Deng, R. Cai, Y. Yu, H. Jiang, C. Wang, J. Li, L. Li, M. Yu, J. Li, L. Xie, Q. Huang, and C. Fan, Adv. Mater. **22**(48), 5473 (2010).

[9]J. Zimmermann, F. A. Reifler, G. Fortunato, L.-C. Gerhardt, and S. Seeger, Adv. Funct. Mater. **18**(22), 3662 (2008).

[10]V. A. Lifton, J. A. Taylor, B. Vyas, P. Kolodner, R. Cirelli, N. Basavanhally, A. Papazian, R. Frahm, S. Simon, and T. Krupenkin, Appl. Phys. Lett. **93**(4), 043112 (2008).

[11]Y. Kwon, N. Patankar, J. Choi, and J. Lee, Langmuir **25**(11), 6129 (2009).

[12]A. K. Gnanappa, D. P. Papageorgiou, E. Gogolides, A. Tserepi, A. G. Papathanasiou, and A. G. Boudouvis, Plasma Processes Polym. **9**(3), 304 (2012).

[13]T. P. N. Nguyen, P. Brunet, Y. Coffinier, and R. Boukherroub, Langmuir **26**(23), 18369 (2010).

[14]F. Lapierre, V. Thomy, Y. Coffinier, R. Blossey, and R. Boukherroub, Langmuir **25**(11), 6551 (2009).

[15]F. Lapierre, P. Brunet, Y. Coffinier, V. Thomy, R. Blossey, and R. Boukherroub, Faraday Discuss. **146**, 125 (2010).

[16]B. Liu and F. F. Lange, J. Colloid Interface Sci. **298**(2), 899 (2006).

[17]T. Deng, K. K. Varanasi, M. Hsu, N. Bhate, C. Keimel, J. Stein, and M. Blohm, Appl. Phys. Lett. **94**(13), 133109 (2009).

[18]C. B. Arnold, P. Serra, and A. Pique, MRS Bull. **32**, 23 (2007).

[19]M. Duocastella, J. M. Fernández-Pradas, J. L. Morenza, and P. Serra, Thin Solid Films **518**(18), 5321 (2010); C. Unger, M. Gruene, L. Koch, J. Koch, and B. N. Chichkov, Appl. Phys. A **103**(2), 271 (2011).

[20]M. S. Brown, N. T. Kattamis, and C. B. Arnold, Microfluid. Nanofluid. **11**(2), 199 (2011); V. Dinca, A. Patrascioiu, J. M. Fernández-Pradas, J. L. Morenza, and P. Serra, Appl. Surf. Sci. **258**(23), 9379 (2012).

[21]V. Dinca, M. Farsari, D. Kafetzopoulos, A. Popescu, M. Dinescu, and C. Fotakis, Thin Solid Films **516**(18), 6504 (2008); L. Rapp, J. Ailuno, A. P. Alloncle, and P. Delaporte, Opt. Express **19**(22), 21563 (2011).

[22]E. Touloupakis, C. Boutopoulos, K. Buonasera, I. Zergioti, and M. T. Giardi, Anal. Bioanal. Chem. **402**(10), 3237 (2012).

[23]C. Boutopoulos, E. Touloupakis, I. Pezzotti, M. T. Giardi, and I. Zergioti, Appl. Phys. Lett. **98**(9), 093703 (2011).

[24]C. Boutopoulos, P. Andreakou, D. Kafetzopoulos, S. Chatzandroulis, and I. Zergioti, Phys. Status Solidi A **205**(11), 2505 (2008).

[25]N. L. Hancox and J. H. Brunton, Philos. Trans. R. Soc. London **260**(1110), 121 (1966).

[26]A. G. Papathanasiou, A. T. Papaioannou, and A. G. Boudouvis, J. Appl. Phys. **103**(3), 034901 (2008).

[27]P. Brunet, F. Lapierre, V. Thomy, Y. Coffinier, and R. Boukherroub, Langmuir **24**(19), 11203 (2008).

[28]L. Feng, Y. Zhang, J. Xi, Y. Zhu, N. Wang, F. Xia, and L. Jiang, Langmuir **24**(8), 4114 (2008).

[29]D. Quere, A. Lafuma, and J. Bico, Nanotechnology **14**(10), 1109 (2003).

[30]M. Reyssat, A. Pépin, F. Marty, Y. Chen, and D. Quéré, Europhys. Lett. **74**(2), 306 (2006); D. Bartolo, F. Bouamrirene, É. Verneuil, A. Buguin, P. Silberzan, and S. Moulinet, Europhys. Lett. **74**(2), 299 (2006).

[31]M. Duocastella, J. M. Fernández-Pradas, P. Serra, and J. L. Morenza, Appl. Phys. A **93**(2), 453 (2008).

[32]V. Scognamiglio, I. Pezzotti, G. Pezzotti, J. Cano, I. Manfredonia, K. Buonasera, F. Arduini, D. Moscone, G. Palleschi, and M. T. Giardi, Anal. Chim. Acta **751**, 161 (2012).